Tunneling Effects on Fine-Structure Splitting in Quantum-Dot Molecules

Hanz Y. Ramírez and Shun-Jen Cheng*

Department of Electrophysics, National Chiao Tung University, Hsinchu 300, Taiwan, Republic of China

(Received 17 March 2009; published 18 May 2010)

We theoretically study the effects of bias-controlled interdot tunneling in vertically coupled quantum dots on the emission properties of spin excitons in various bias-controlled tunneling regimes. As a main result, we predict substantial reduction of optical fine-structure splitting without any drop in the optical oscillator strength for the coupled dots with high tunneling rates. This special reduction diminishes the distinguishability of polarized decay paths in cascade emission processes suggesting the use of stacked quantum-dot molecules as entangled photon-pair sources.

DOI: 10.1103/PhysRevLett.104.206402 PACS numbers: 71.45.Gm, 03.67.Bg, 78.55.Cr, 78.67.Hc

Tunneling is a remarkable quantum property of microscopic particles that has no classical counterpart, which allows coupling between two objects spatially separated by a finite potential barrier. Recent examples of tunnel effects in coupled quantum-dot (QD) systems include the tunability of fluctuations in Kondo currents [1], reduction of electronic spin decoherence by interaction with nuclear spin [2], conditional dynamics of transitions [3], and bias control of g tensors [4].

Currently, a highly desirable feature of QD-based photon emitters is the reduced fine-structure splitting (FSS) between the intermediate one-exciton spin states [5]. The FSSs (typically $\sim 10^1$-10^2 μeV, greater than the intrinsic broadening of emission line ~ 1 μeV) make the two possible decay paths in biexciton cascade processes energetically distinguishable, and have become a main obstacle in the production of polarization-entangled photon pairs from QDs [6–10]. Researchers have recently demonstrated significant reductions in the FSSs of single QDs using strain and postannealing techniques, and the application of electric and magnetic fields [11–13]. In most experiments, however, it is not clear if the reduction of FSS is caused by the undoing of symmetry breaking or the reduction of e-h wave function overlap. The latter effect reduces not only the FSS but also the oscillator strength of e-h recombination, yielding narrow intrinsic radiative broadening and actually inhibiting the generation of entangled photon pairs [14,15].

In this Letter, we theoretically examine the effects of quantum tunneling in vertical QD molecules on the optical fine-structure properties by using the (partial) configuration interaction (PCI) method. Remarkably, we predict a significant reduction of the optical FSSs in coupled double quantum dots (DQDs) with high tunneling rates, without any decrease in the optical oscillator strength.

Let us consider a pair of vertically stacked quantum dots along the growth z axis, separated by an interdot distance d and subject to an applied electric field F, as shown in Fig. 1(a) [16]. The e-h Hamiltonian for a single spin exciton in a coupled double QD is written as

$$\begin{aligned} H = & \sum_{j,\sigma} (\varepsilon_j^e + eFz_j) c_{j\sigma}^\dagger c_{j\sigma} + \sum_{n,\chi} (\varepsilon_n^h - eFz_n) h_{n\chi}^\dagger h_{n\chi} \\ & - \sum_{j\in L, k\in R, \sigma} t_{jk}^e (c_{j\sigma}^\dagger c_{k\sigma} + c_{k\sigma}^\dagger c_{j\sigma}) \\ & - \sum_{n\in L, m\in R, \chi} t_{nm}^h (h_{n\chi}^\dagger h_{m\chi} + h_{m\chi}^\dagger h_{n\chi}) \\ & - \sum_{kmnj,\sigma\chi} V_{kmnj}^{e\text{-}h} c_{k\sigma}^\dagger h_{m\chi}^\dagger h_{n\chi} c_{j\sigma} \\ & + \sum_{kmnj,\sigma\chi\chi'\sigma'} V_{k\sigma,m\chi,n\chi',j\sigma'}^{e\text{-}h\ \mathrm{exch}} c_{k\sigma}^\dagger h_{m\chi}^\dagger h_{n\chi'} c_{j\sigma'}, \end{aligned} \tag{1}$$

where the composite indexes j, k (n, m) denote the electron (valence hole) orbitals and dot positions [L (R) for the left (right) dot], $\sigma = \uparrow$ or $\downarrow$ ($\chi = \Uparrow$ or $\Downarrow$) represents electron (hole) spin with $s_z = \frac{1}{2}$ or $-\frac{1}{2}$ ($j_z = \frac{3}{2}$ or $-\frac{3}{2}$), $c_{j\sigma}^\dagger$ and $c_{j\sigma}$ ($h_{n\chi}^\dagger$ and $h_{n\chi}$) are the electron (hole) creation and annihilation operators, respectively, ε_i^e (ε_n^h) is the kinetic energy of an electron (a valence hole), e is the unit charge, and $z_{j\in L} = 0$ ($z_{j\in R} = d$) is the z position of the left (right)

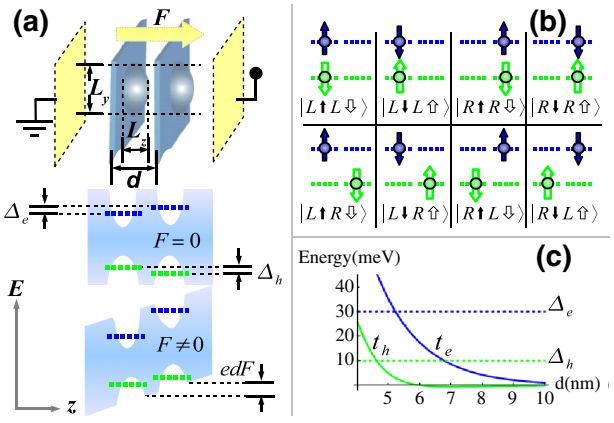

FIG. 1 (color online). Schematic diagrams of (a) a double QD structure and (b) spin-exciton configurations. (c) The calculated hopping parameters, t_e (blue) and t_h (green), vs interdot distance d. Horizontal dashed lines: the values of Δ_e and Δ_h considered throughout this work.

 © 2010 The American Physical Society

dot. Here, the valence hole orbitals of the highly quantized strained dots are assumed to be purely heavy-hole-like. The terms with the hopping parameters (t^e_{jk}, t^h_{nm}) describe the (spin-conserved) carrier tunneling between adjacent dots. The matrix elements of conventional e-h Coulomb interaction and the e-h exchange interactions are $V^{e\text{-}h}_{kmnj} \equiv \iint d^3r_1 d^3r_2 \Phi^{e*}_k(\vec{r}_1)\Phi^{h*}_m(\vec{r}_2)(e^2/4\pi\epsilon r_{12})\Phi^h_n(\vec{r}_2)\Phi^e_j(\vec{r}_1)$ and $V^{e\text{-}h\,\mathrm{exch}}_{k\sigma,m\chi,n\chi',j\sigma'} \equiv \iint d^3r_1 d^3r_2 \Phi^{e*}_k(\vec{r}_1)u^*_{c\sigma}(\vec{r}_1)\Phi^h_m(\vec{r}_1)u_{v\chi}(\vec{r}_1)(e^2/4\pi\epsilon r_{12})\Phi^{h*}_n(\vec{r}_2)u^*_{v\chi'}(\vec{r}_2)\Phi^e_j(\vec{r}_2)u_{c\sigma'}(\vec{r}_2)$, respectively, where Φ_α are single-particle envelope wave functions, $u_{c\sigma}$ ($u_{v\chi}$) are the electron (hole) Bloch functions, ϵ is the dielectric constant and $r_{12} \equiv |\vec{r}_1 - \vec{r}_2|$. Within the dipole-dipole approximation, the long-range part of the e-h exchange interaction is given by $V^{e\text{-}h\,\mathrm{exch(LR)}}_{kmnj} \equiv \delta^{kmnj}_1 \approx [3e^2\hbar^2 E_p/(4\pi\epsilon)4m_0E_g^2]\iint d^3\vec{r}_1 d^3\vec{r}_2 \Phi^{e*}_k(\vec{r}_1) \times \Phi^h_m(\vec{r}_1)\Phi^{h*}_n(\vec{r}_2)\Phi^e_j(\vec{r}_2)[(y_1-y_2)^2 - (x_1-x_2)^2 + 2i(x_1-x_2)(y_1-y_2)]/(r_{12})^5$, where E_p is the conduction-valence band interaction energy [17], E_g the band gap energy, and m_0 the mass of a free electron [18]. The energy spectrum of an interacting exciton in a DQD can be calculated by direct diagonalization of Eq. (1) in the basis of exciton configurations constructed from the all S and P orbitals of individual dots [19].

Besides the fully numerical approach, the following analysis is performed using a simplified "rigid orbital" model to improve physical understanding. Based on the lowest single-particle orbitals of single dots, eight spin-exciton configurations are constructed, as displayed in Fig. 1(b). To analyze further the (linear) polarization of emitted light, a new basis is defined by the linear transformation of the configurations according to the parity symmetry: $|LL\pm\rangle \equiv \frac{1}{\sqrt{2}}(|L\uparrow L\Downarrow\rangle \pm |L\downarrow L\Uparrow\rangle)$, $|RR\pm\rangle \equiv \frac{1}{\sqrt{2}}(|R\uparrow R\Downarrow\rangle \pm |R\downarrow R\Uparrow\rangle)$, $|LR\pm\rangle \equiv \frac{1}{\sqrt{2}}(|L\uparrow R\Downarrow\rangle \pm |L\downarrow R\Uparrow\rangle)$, $|RL\pm\rangle \equiv \frac{1}{\sqrt{2}}(|R\uparrow L\Downarrow\rangle \pm |R\downarrow L\Uparrow\rangle)$. Notably, only the configurations with positive (negative) parity are associated with a π_x- (π_y-)polarized light emission. In the basis ordered by $|LL\pm\rangle$, $|RR\pm\rangle$, $|LR\pm\rangle$, $|RL\pm\rangle$, the decoupled 4×4 Hamiltonian matrix is

$$\hat{H}_\pm = \begin{pmatrix} -V_{e\text{-}h} \pm \delta_{DD} & \pm\delta_{\mathrm{II}} & -t_h & -t_e \\ \pm\delta_{\mathrm{II}} & -V_{e\text{-}h} + \Delta_e + \Delta_h \pm \delta_{DD} & -t_e & -t_h \\ -t_h & -t_e & -eFd + \Delta_h \pm \delta_{\mathrm{II}} & \pm\delta_{\mathrm{II}} \\ -t_e & -t_h & \pm\delta_{\mathrm{II}} & eFd + \Delta_e \pm \delta_{\mathrm{II}} \end{pmatrix}, \tag{2}$$

where the kinetic energy offset $\varepsilon^e_L + \varepsilon^h_L$ is removed for brevity, $\Delta_{(e)\,h} \equiv \varepsilon^{(e)\,h}_R - \varepsilon^{(e)\,h}_L$ denotes the difference between kinetic energies of the two adjacent dots due to the inevitable slight differences in size, shape, or chemical composition, $V_{e\text{-}h} \equiv V^{e\text{-}h}_{LLLL} = V^{e\text{-}h}_{RRRR}$ denotes the direct Coulomb interaction between an e-h pair in the same single dot, and $\delta_{DD} \equiv \delta^{RRRR}_1 = \delta^{LLLL}_1$ ($\delta_{\mathrm{II}} \equiv \delta^{LRRL}_1 = \delta^{RLLR}_1 \approx \delta^{LLRR}_1 = \delta^{RRLL}_1$) is the long-range e-h exchange interaction in a direct exciton (an indirect exciton). Within the three-dimensional parabolic model for the confining potentials of single QDs, the single-particle wave functions of the lowest orbitals of single dots can be described by $\Phi_{L/R}(x,y,z) = (\pi^{3/2}l_xl_yl_z)^{-1/2} \times \exp\{-\frac{1}{2}[(\frac{x}{l_x})^2 + (\frac{y}{l_y})^2 + (\frac{z-z_{L/R}}{l_z})^2]\}$, characterized by the wave function extents $l_{\alpha=x,y,z}$. Accordingly, we derive $V_{e\text{-}h} \approx \frac{e^2}{4\pi\epsilon}\frac{1}{l}\{[\sqrt{2}\sin^{-1}(\sqrt{1-a^2})]/[\sqrt{\pi}(\sqrt{1-a^2})]\}$, $\delta_{DD} = \{(3\sqrt{\pi}e^2\hbar^2E_p)/[(4\pi\epsilon)16\sqrt{2}m_0E_g^2]\}[(l_y - l_x)/l_x^2l_y^2] \times e^{(3\sqrt{\pi}/4)^2(l_z/l_y)^2}\mathrm{erfc}[(3\sqrt{\pi}/4)(l_z/l_y)]$, [18,20,21] and $\delta_{\mathrm{II}} = \delta_{DD}e^{-(d^2/2l_z^2)}$, for a slightly deformed DQD ($\xi \equiv \frac{l_y-l_x}{l_y} \ll 1 \neq 0$, where $l \equiv (l_x+l_y)/2$, $a \equiv l_z/l$). The parameters t_e are evaluated using a standard exponential model [22] and fitted to the results of pseudopotential calculations in Ref. [23]. For the evaluation of t_h, we follow the formulation in Ref. [24] derived from the four band Luttinger-Kohn model with the consideration of spin-orbit coupling.

The energy spectrum $\{E_{\pi_x,i}\}$ ($\{E_{\pi_y,i}\}$) of the exciton states $|\pi_x;i\rangle$ ($|\pi_y;i\rangle$) as the initial states of the π_x- (π_y)-polarized light emission is calculated by diagonalizing H_+ (H_-) in Eq. (2) [25]. In the combined energy spectrum, $\{E_{\pi_x,i}, E_{\pi_y,i}\}$, each level is a doublet of the spin-exciton states, $|\pi_x;i\rangle$ and $|\pi_y;i\rangle$, which are split by an FSS $\Delta E_i \equiv E_{\pi_y,i} - E_{\pi_x,i}$ [inset of Fig. 2(a)]. The π_x- (π_y)-linear-polarized photoluminescence (PL) spectra are obtained using Fermi's golden rule: $I_{x(y)}(\omega) = \sum_i F(E_i,T)|\langle 0|P^-_{x(y)}|\pi_x(\pi_y);i\rangle|^2\delta(E_{\pi_x(\pi_y),i} - \hbar\omega)$, where the subscript i denotes initial states of the PL transition, ω is the frequency of the emitted photon, the

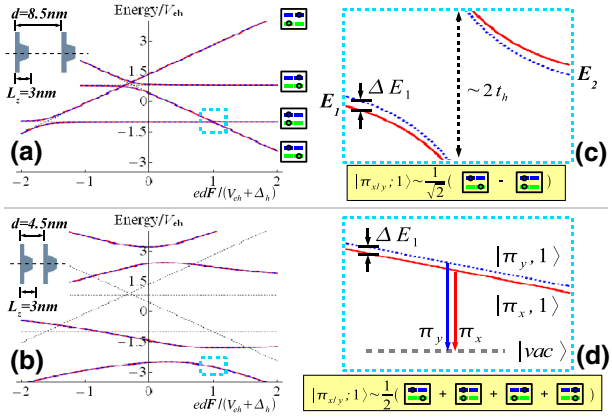

FIG. 2 (color online). Calculated energy spectra vs bias field F of (a) a DQD with $d = 8.5$ nm and (b) a DQD with $d = 4.5$ nm. Straight dashed lines describe the energy spectrum of a decoupled DQD. (c) and (d) are magnified fine structures of the corresponding energy spectra (a) and (b), at near resonance, and the (schematic) configuration intermixings of the lowest exciton states.

operator $P_x^{(-)} = \sum_{n,j} S_{n,j}(h_{n\Uparrow} c_{j\downarrow} + h_{n\Downarrow} c_{j\uparrow})$ $[P_y^{(-)} = -i\sum_{n,j} S_{n,j}(h_{n\Uparrow} c_{j\downarrow} - h_{n\Downarrow} c_{j\uparrow})]$ describes the all possible e-h recombinations that produce the $\pi_x[\pi_y]$ linear polarized PL, $S_{n,j} = \int d^3 r \Phi_n^{h*}(\vec{r}) \Phi_j^e(\vec{r})$ is the e- and h-wave function overlap, and $F(E_i, T) = \exp(-E_i/k_B T)/[\sum_l \exp(-E_l/k_B T)]$ is the probability of occupation of state $|i\rangle$, where k_B is the Boltzmann constant and T is temperature.

Figure 2(a) shows the calculated energy spectra of a coupled DQD with $d = 8.5$ nm under various applied biases. Under the weak tunneling (WT) condition (defined by $t_{e\,(h)}/\Delta_{e\,(h)} \ll 1$), the 4×4 Hamiltonian matrix, Eq. (2), can be decomposed into two 2×2 blocks that are coupled only by relatively weak electron hopping. Thus, the Hamiltonian matrix for the two lowest spin-exciton states can be approximated as the following 2×2 block:

$$\hat{H}_{\pm}^{\mathrm{WT}} = \begin{pmatrix} -V_{e\text{-}h} \pm \delta_{DD} & -t_h \\ -t_h & -eFd + \Delta_h \pm \delta_{DD} \end{pmatrix}, \quad (3)$$

with respect to the basis $|LL\pm\rangle$ and $|LR\pm\rangle$. Equation (3) is actually equivalent to the widely used solvable three-orbital model for DQDs [26]. The eigenstates of Eq. (3) are superpositions of the optically active exciton configuration $|LL\pm\rangle$ and the inactive configuration $|LR\pm\rangle$, determined by the bias-controlled detuning from resonance ($|edF - (\Delta_h + V_{e\text{-}h})|$). Expanding the exciton eigenstates in the used basis for Eq. (2), i.e., $|\pi_x; i\rangle = \sum_{nj} C^x_{nj,i} |nj+\rangle$ and $|\pi_y; i\rangle = \sum_{nj} C^y_{nj,i} |nj-\rangle$, the intensities and the FSS associated with the lowest spectral lines are given by $I_1 \approx F(E_1, T)(C_{LL,1} S_D + C_{LR,1} S_I)^2$ and $\Delta E_1 \approx 2(C^2_{LL,1}\delta_{DD} + C^2_{LR,1}\delta_{II})$, where $C_{LL,1} \equiv C^x_{LL,1} = C^y_{LL,1}$ ($C_{LR,1} \equiv C^x_{LR,1} = C^y_{LR,1}$) are the expansion coefficients associated with the bright (dark) exciton configurations $|LL\pm\rangle$ ($|LR\pm\rangle$) and $S_D \equiv S_{LL} = S_{RR} \approx 1$ ($S_I \equiv S_{LR} = S_{RL} = e^{-(d^2/4l_z^2)}$) is the e-h wave function overlap in a direct-exciton (an indirect-exciton) configuration. Accordingly, both the I_1 and the ΔE_1 of a weakly spatially coupled DQD in the weak tunneling regime ($S_I \ll S_D$ and $\delta_{II} \ll \delta_{DD}$) are mainly proportional to $C^2_{LL,1}$ and should depend similarly on applied bias fields. Figure 3 presents the calculated F dependences of the I_1 and ΔE_1, and selected polarized PL spectra of the DQD in the fields near resonance, obtained using the PCI method. The results obtained using the model Eq. (2) are also presented in Fig. 3(a) for comparison. Both sets of results show similar features that are consistent with the analysis presented above. The only remarkable difference is that the magnitude of the resonance field obtained using the PCI method is smaller than that from the simple model because of the reduced indirect-exciton energy by the interdot Coulomb attraction.

At very low bias ($|edF/(V_{e\text{-}h} + \Delta_h)| \ll 1$), the ground states of the exciton are $|\pi_x; 1\rangle \approx |LL+\rangle$ and $|\pi_y; 1\rangle \approx |LL-\rangle$. The intensity (FSS) of the corresponding linear polarized emission lines is $I_1 \approx (S_D)^2$ ($\Delta E_1 \approx 2\delta_{DD}$), approaching the value of the intensity (FSS) of the lowest

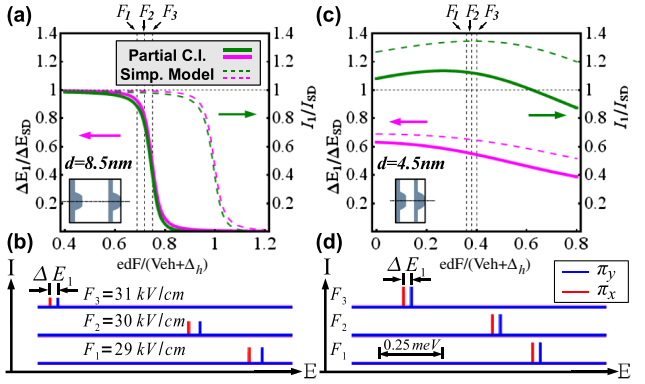

FIG. 3 (color online). (a) Calculated normalized FSS $\Delta E_1/\Delta E_{\mathrm{SD}}$ [light (magenta) lines] and intensity I_1/I_{SD} [dark (green) lines] of the main PL spectral lines of the DQD with $d = 8.5$ nm as functions of F, where ΔE_{SD} (I_{SD}) denotes the FSS (PL intensity) for a single dot. Solid (dashed) lines show the results calculated by using the PCI method [the simple model of Eq. (2)]. (b) Selected polarized PL spectra for the considered DQD in (a) under the fields F_i around resonance at $T = 10$ K. (c) and (d) The same calculated results as (a) and (b) but for the DQD with short interdot distance $d = 4.5$ nm.

spectral lines of a single dot, I_{SD} (ΔE_{SD}). At near resonance ($edF/(V_{e\text{-}h} + \Delta_h) \approx 1$), where $|\pi_x; 1\rangle \approx \frac{1}{\sqrt{2}}(|LL+\rangle - |LR+\rangle)$ and $|\pi_y; 1\rangle \approx \frac{1}{\sqrt{2}}(|LL-\rangle - |LR-\rangle)$, only the hole in the exciton can be transferred between dots while the electron is stably localized in the left dot. The intensity (FSS) of the corresponding polarized emission lines is $I_1 \approx (S_D + S_I)^2/2$ ($\Delta E_1 \approx \delta_{DD} + \delta_{II}$), which is only about 50% of that for a single dot. The resonant interdot tunneling of a single hole significantly reduces the overlap of the electron and hole wave functions, leading to not only the decrease in the optical FSS but also the oscillator strength of an e-h recombination. The decreased oscillator strength of e-h recombination reduces the intrinsic broadening width of the main exciton lines. Thus, such a FSS reduction does not support the feasibility of the dot-based entangled photon-pair source devices [27,28].

Figure 2(b) shows the energy spectra of a coupled DQD with smaller $d = 4.5$ nm. Figure 3(c) plots the normalized I_1 and ΔE_1 of the lowest spectral lines vs F. Generally, the strongly coupled DQDs have smaller FSS ΔE_1 but larger I_1 than single dots or weakly coupled dot molecules, since small interdot distance makes $t_{e\,(h)}$ greater than $\Delta_{e\,(h)}$ and the interdot tunneling more likely. In the strong tunneling (ST) limit ($t_\beta \gg \Delta_\beta$), both electrons and holes can be transferred between dots over a very wide range of detuning. Thus, Eq. (2) can be approximated to

$$\hat{H}_{\pm}^{\mathrm{ST}} \approx \begin{pmatrix} 0 & 0 & -t_h & -t_e \\ 0 & 0 & -t_e & -t_h \\ -t_h & -t_e & 0 & 0 \\ -t_e & -t_h & 0 & 0 \end{pmatrix}. \quad (4)$$

The lowest eigenstates for Eq. (4) are $\frac{1}{2}(|LL\pm\rangle + |RR\pm\rangle + |LR\pm\rangle + |RL\pm\rangle)$, highly intermixing all exciton

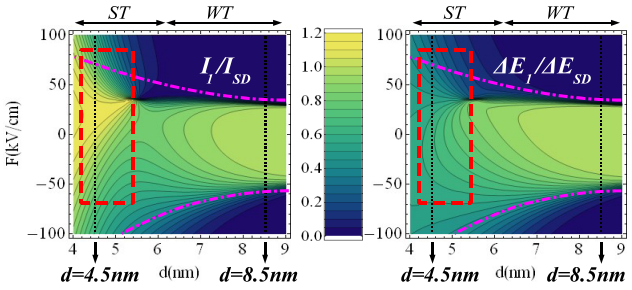

FIG. 4 (color online). Normalized intensity I_1/I_{SD} (left) and FSS $\Delta E_1/\Delta E_{\mathrm{SD}}$ (right) of the lowest PL spectral lines of coupled DQDs, as functions of d and F, obtained from the PCI calculation. The red dashed line boxes highlight the feature of reduced ΔE_1 and increased I_1 of the DQDs with short d. The vertical dotted lines indicate $d = 4.5$ nm and $d = 8.5$ nm for which Figs. 2 and 3 are calculated. The magenta dash-dotted line in the upper (lower) half plane indicates the hole (electron) resonance.

configurations. This indicates that both kinds of particles, electrons and holes, in the eigenstates are likely delocalized and can be simultaneously transferred between the coupled dots. Accordingly, we have $I_1 \approx (S_D + S_I)^2$ and $\Delta E_1 \approx \delta_{DD} + 2\delta_{\mathrm{II}}$, i.e., that the FSS is only about one-half of the magnitude of ΔE_{SD} but the intensity of the polarized emission lines is slightly larger than I_{SD}. In the ST regime, not only valence holes but also electrons are spread over the two coupled dots. The simultaneous e and h resonant transfer between dots enlarges the optically active volume and increases the mean distance $\langle r_{12}\rangle$ in the long-ranged e-h exchange interactions, resulting in the larger I_1 and smaller ΔE_1. In Fig. 3(c), the PCI results reveal a similar feature but smaller magnitudes of I and FSS than the model Eq. (2). This is because the components of indirect exciton, which are mixed in the radiative exciton states, are increased by the interdot Coulomb attraction that is associated with both Coulomb direct and correlation interactions.

Figure 4 plots the normalized I_1 and ΔE_1 (by I_{SD} and ΔE_{SD}) of DQDs versus the d and F, obtained from the PCI calculation. In the WT regime, as discussed previously, I_1 and ΔE_1 depend similarly on F. As a DQD is driven into the ST regime, I_1 are markedly increased and the FSS is reduced to only $\sim$50% of ΔE_{SD} (see the regions highlighted by dashed-line boxes) [16]. This finding suggests that in a dot ensemble the number of useful dots with sufficiently small FSSs that are suitable for fabricating devices can be roughly doubled if such devices are made of double QD structures. The increased I_1 and reduced ΔE_1 are robust against the detuning, being almost insensitive to F. The values of $\Delta_e = 30$ meV and $\Delta_h = 10$ meV, are estimated for a pair of dots with around 1–2 monolayer difference in height. Whether double QDs can be easily prepared in the ST regime, and the strong tunneling effect can be subsequently exploited, depends on the ratios $t_e/\Delta_e \geq 1$ and $t_h/\Delta h \geq 1$. Fabricating more similar dots can increase the ratios t_e/Δ_e and t_h/Δ_h [29], and makes the device more efficient.

In summary, this study discusses the effects of quantum tunneling on polarized photon emission from spin excitons in vertically stacked double quantum dots. Results show that an increase in the optically active volume and charge delocalization via quantum tunneling inhibits the optical FSS of coupled QDs in the strong tunneling regime without any decrease in the optical oscillation strength. This tunneling-driven FSS reduction makes strongly coupled vertical quantum-dot molecules better sources of entangled photon pairs than single dots.

The authors would like to thank the NSC of Taiwan for support. Wen-Hao Chang (NCTU) is appreciated for his valuable discussions.

*sjcheng@mail.nctu.edu.tw

[1] D. T. McClure *et al.*, Phys. Rev. Lett. **98**, 056801 (2007).
[2] D. J. Reilly *et al.*, Phys. Rev. Lett. **101**, 236803 (2008).
[3] L. Robledo *et al.*, Science **320**, 772 (2008).
[4] T. Andlauer and P. Vogl, Phys. Rev. B **79**, 045307 (2009).
[5] A. S. Bracker *et al.*, Semicond. Sci. Technol. **23**, 114 004 (2008), and references therein.
[6] C. Santori *et al.*, Phys. Rev. B **66**, 045308 (2002).
[7] N. Akopian *et al.*, Phys. Rev. Lett. **96**, 130501 (2006).
[8] L. He *et al.*, Phys. Rev. Lett. **101**, 157405 (2008).
[9] R. J. Young *et al.*, Phys. Rev. Lett. **102**, 030406 (2009).
[10] R. Singh and G. Bester, Phys. Rev. Lett. **103**, 063601 (2009).
[11] W. Langbein *et al.*, Phys. Rev. B **69**, 161301(R) (2004).
[12] R. M. Stevenson *et al.*, Nature (London) **439**, 179 (2006).
[13] M. Reimer *et al.*, Phys. Rev. B **78**, 195301 (2008).
[14] A. Greilich *et al.*, Phys. Rev. B **73**, 045323 (2006).
[15] K. Kowalika *et al.*, Appl. Phys. Lett. **91**, 183 104 (2007).
[16] W. H. Chang *et al.*, Phys. Rev. B **77**, 245314 (2008).
[17] $E_p \equiv 2p_{\mathrm{vc}}^2/m_0$, where $p_{\mathrm{vc}} = \langle S|\hat{\tilde{p}}|X\rangle$ is the conduction-valence interband linear momentum matrix element.
[18] E. Poem *et al.*, Phys. Rev. B **76**, 235304 (2007).
[19] See supplementary material at http://link.aps.org/supplemental/10.1103/PhysRevLett.104.206402 for details of the implementation of the PCI calculation.
[20] M. Glazov *et al.*, Phys. Rev. B **76**, 193313 (2007).
[21] J. L. Zhu *et al.*, Appl. Phys. Lett. **90**, 261 119 (2007).
[22] F. Vasko and A. Kuznetsov, *Electronic States and Optical Transitions in Semiconductor Heterostructures* (Springer-Verlag, New York, 1999), p. 75.
[23] G. Bester, J. Shumway, and A. Zunger, Phys. Rev. Lett. **93**, 047401 (2004).
[24] J. I. Climente *et al.*, Phys. Rev. B **78**, 115323 (2008).
[25] $l_x = 5.3$ nm, $l_y = 5$ nm and $l_z = 1.5$ nm are taken for the QDs considered throughout this work.
[26] E. A. Stinaff *et al.*, Science **311**, 636 (2006).
[27] R. Hafenbrak *et al.*, New J. Phys. **9**, 315 (2007).
[28] A. J. Hudson *et al.*, Phys. Rev. Lett. **99**, 266802 (2007).
[29] A. S. Bracker, J. Shumway, and A. Zunger, Appl. Phys. Lett. **89**, 233 110 (2006).